Available online at www.sciencedirect.com

SciVerse ScienceDirect

http://www.elsevier.com/locate/biombioe

A new innovative CFD-based optimisation method for biomass combustion plants

Ali Shiehnejadhesar [a,b,*], Kai Schulze [a], Robert Scharler [a,b,c], Ingwald Obernberger [a,b,c]

[a] Bioenergy 2020+GmbH, Inffelgasse 21b, 8010 Graz, Austria
[b] Institute for Process and Particle Engineering, Graz University of Technology, Inffeldgasse 21b, 8010 Graz, Austria
[c] BIOS BIOENERGIESYSTEME GmbH, Inffeldgasse 21b, 8010 Graz, Austria

ARTICLE INFO

Article history:
Received 27 June 2012
Received in revised form
29 January 2013
Accepted 3 February 2013
Available online 11 March 2013

Keywords:
CFD
Optimisation
Combustion
Biomass
Emission reduction

ABSTRACT

In this paper, the work on the development and test of a basic design tool for the automatic performance of parameter studies for the optimisation of biomass combustion plants is presented. The model consists of parameterisation and optimisation routines linked with an in-house developed empirical packed bed combustion model as well as gas phase CFD models especially adapted for biomass grate furnaces.

To test and verify the routine developed, it has been applied to the optimisation of a 180 kW_{th} pilot-scale grate furnace. The main focus was on the minimisation of CO emissions and the pressure loss by changing the diameter and angle of the secondary air nozzles. The simulation results show that the time of the optimisation process can be reduced considerably by the automatic routine developed and the evaluation of several independent design parameters is possible. This new procedure forms an important milestone towards automatic CFD-based furnace and boiler optimisations in the future.

1. Introduction

CFD models are being successfully applied for the simulation of biomass combustion plants in order to design and improve the plants with respect to lower CO emissions, the reduction of flue gas temperature peaks, additionally increased plant efficiencies. However, even experienced scientific personnel needs a large number of time-consuming simulations during a CFD-based design cycle. A "real" optimum typically cannot be found due to the complex interactions of the influencing parameters in the plant. While automatic CFD-optimisation methods have been applied for the design of cyclones [1–4], the combustion chamber of engines [5,6] and in the field of turbo machinery [7–9], only manual optimisation methods have been applied in the field of biomass combustion plants [10–12] due to the high degree of complexity of the processes in the plant and thus the high number of influencing parameters.

Therefore, at BIOENERGY 2020+ a tool for the automatic CFD-optimisation of biomass grate furnaces has been developed. The model consists of parameterisation and optimisation routines linked with an in-house developed model for biomass grate furnaces (empirical packed bed combustion model and gas phase CFD models especially adapted for biomass combustion). In order to test and verify the efficiency of the routine developed, the procedure has been applied to a pilot-scale grate furnace (180 kW_{th}). The main focus was on the minimisation of carbon monoxide emissions and the energy demand of the secondary air fan by changing the diameter and angle of the secondary air nozzles.

* *Corresponding author*. Institute for Process and Particle Engineering, Graz University of Technology, Inffeldgasse 21b, 8010 Graz, Steiermark, Austria. Tel.: +43 316 8739230; fax: +43 316 8739202.
E-mail addresses: ali.shienejadhesar@gmail.com, ali.shiehnejad@bioenergy2020.eu (A. Shiehnejadhesar).
0961-9534/$ – see front matter
http://dx.doi.org/10.1016/j.biombioe.2013.02.005

2. Methodology

As already explained, parameterisation routines and optimisation functions have been linked with an in-house developed model for biomass grate furnaces (empirical packed bed combustion model and gas phase CFD models especially adapted for biomass combustion).

2.1. *CFD model for biomass grate furnaces*

An empirical model was developed for the description of solid biomass combustion on the grate [13–15]. The model describes the mass and energy fluxes on the grate as boundary conditions for the following CFD simulation of the turbulent reactive flow in the combustion chamber. The empirical packed bed combustion model consists of three parts:

- 1D-profiles along the grate, which describe fuel drying and the thermal degradation of the fuel components C, H, O as well as profiles of the primary air and re-circulated flue gas supplied below the grate are the basis of the model.
- By the definition of conversion parameters based on literature data and experiments, which describe the conversion of the fuel components C, H, and O to the flue gas components CH_4, CO, CO_2, H_2, H_2O and O_2 which are dependent on the local fuel composition and the stoichiometric air ratio on the grate. Then the local composition of the flue gas released from the packed bed can be described. Nitrogen species have not been considered since the CFD simulation of NO_x formation was not within the scope of this work.
- Finally, the local mass and energy profiles and hence, the profiles of flue gas velocity, temperature and composition along the grate are calculated.

The results of the simulation applications (e.g. Refs. [13,16–19]) showed that the empirical packed bed combustion model is sufficiently accurate for the calculation of the boundary conditions for the CFD simulation of flow and gas phase combustion in the furnace. However, it is noted that the processes of solid biomass combustion on the grate cannot be described by the empirical packed bed combustion model. For the simulation of the gas phase, the Realizable $k-\varepsilon$ Model for turbulence, the Discrete Ordinates Model for radiation and the Eddy Dissipation Model (EDM) by Magnussen and Hjertager [20] in combination with a global methane 3-step mechanism (CH_4, CO, H_2, CO_2, H_2O, O_2) [21] are applied. The sub-models and the gas phase models together with the empirical packed bed combustion model have been experimentally validated [13,15] and successfully applied for several plants.

2.2. *Selection of the design parameters*

The secondary air nozzles are of special importance when designing and optimising a biomass furnace. They are the key factor for efficient air staging without backflow in the primary combustion zone (NO_x reduction by primary measures), for a good turbulent mixing and CO burnout, to reduce furnace volume and to lower the amount of excess air (increased efficiency). Therefore, the diameter and the angle of the secondary air nozzles have been selected as design parameters in order to achieve the best geometric configuration concerning low CO emissions and pressure losses over the secondary air nozzles.

2.3. *Optimisation function*

A weight function has to be defined to combine the two optimisation variables (CO emissions and pressure loss over the secondary air nozzles) according to their relevance in a common function. While the energy demand of the fan linearly increases with the pressure loss over the secondary air nozzles, the relevance of the CO emissions substantially increases if a certain level of CO emissions is exceeded. Equation (1) shows the weight function:

$$W = A \cdot \left(\frac{1}{Y_{CO}}\right)^{\gamma} + B \cdot \Delta P \quad (1)$$

where W is the weight function, Y_{CO} is the CO mole fraction ($\mu L\ L^{-1}$), A, γ and B are constant values and ΔP is the pressure loss (Pa).

Here, for the pressure drop a linear correlation to the weight function has been assumed (proportional to the energy demand of the fan). Regarding the CO emissions, a polynomial function with a strong increase at a chosen emission limit (20 $\mu L\ L^{-1}$ in the present case) was supposed.

The constants A and B of the second order polynomial function ($\gamma = -2$) have been determined in a way to achieve roughly the same contribution of the pressure loss and the CO emission to the weight function at the respective limits of the output variables ($\Delta P = 2500$ Pa – maximum allowable pressure for fan design; CO emissions = 20 $\mu L\ L^{-1}$ – emission limit). The values for the constants are given in Table 1.

Within the optimisation process the design parameters are varied and evaluated using the weight function. The optimisation cycle for a selected combination of design parameters works as following:

- Parameterisation of the geometry and definition of design points based on design parameters selected (the variation range of the design parameters is shown in Table 2)
- Automatic performance of CFD simulations with ANSYS® FLUENT® for the defined design points within the ANSYS® Workbench™
- Evaluation of the output variables and calculation of the weight function for the design points
- Minimisation of the weight function to find the optimum geometric configuration (input parameters)

Table 1 – Values of the model constants used in the weight function.

Constant	Value	Units
A	10	Consistent unit $(\mu L\ L^{-1})^{-2}$
γ	−2	–
B	1	Consistent unit (Pa^{-1})

Table 2 – Design parameters and their variation range.

Design parameter	Range
Diameter (mm)	10–35
Angle (deg)	1–30

2.4. *Case study description*

To investigate the efficiency of the method developed, a design optimisation for a pilot-scale moving grate furnace equipped with a hot water fire tube boiler (180 kW_{th}) using Miscanthus as fuel has been carried out. Table 3 provides the most relevant operating conditions of the furnace and the fuel composition.

Fig. 1 illustrates the different sections of the biomass combustion plant considered. The simulation domain comprises the combustion chamber from above the fuel bed up to the exit of the radiative fire tube. While the primary combustion zone is equipped with six flue gas recirculation nozzles, eight secondary air nozzles are located at the entrance of the secondary air combustion chamber.

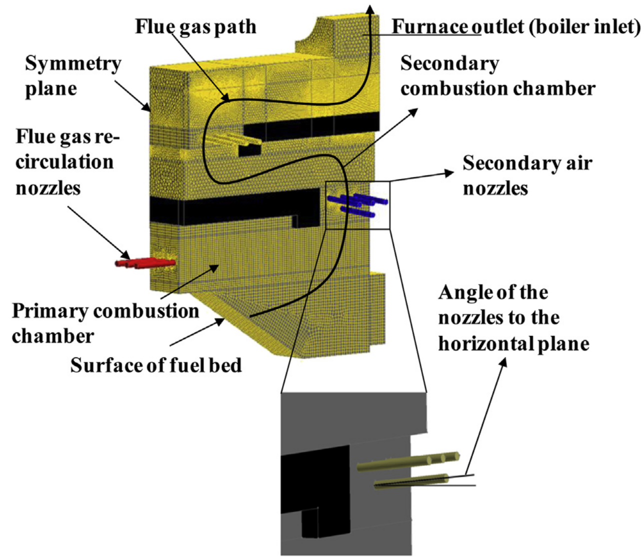

Fig. 1 – Geometry and computational grid of the pilot-scale grate furnace (top) as well as design parameters (nozzles angle to the wall and diameter) (bottom).

3. Results and discussion

To verify the efficiency of the optimisation strategy concerning the reduction of the overall time for the performance of the case study in comparison to conventional manual methods, at first a manual optimisation run was carried out (as a reference). Since this method is very time-consuming, only the diameter of the nozzles has been changed (for 10 design points). A computational grid with 700,000 cells in total was used in the manual optimisation study. In the next step, the automatic optimisation routine was performed for the two selected design parameters for 80 design points. The number of computational cells was about 1 million for the automatic optimisation study using the tetrahedral cell type. Figs. 2 and 3 show the calculated results concerning CO emissions and pressure losses for the manual and the automatic optimisation method. The black circles in the diagrams represent the evaluated design points within the automatic CFD simulations for each pair of design parameters (diameter and angle). The red line (in the web version) in the diagrams represents the results obtained with the manual optimisation method. Based on the results of the automatic CFD simulation (black circles), a response surface was created by a second order polynomial fit. The trends for both methods generally are in good agreement for comparable design points.

Next, a sensitivity analysis has been carried out to outline and evaluate the impact of the input design parameters on the output variables (CO emission, pressure loss). According to Ref. [22], the single parameter sensitivities are defined as the

Table 3 – Operating conditions and fuel characteristics of the pilot-scale grate furnace.

	Unit	Value
Operating conditions		
Boiler load	kW_{th}	180
Adiabatic flame temperature	°C	937
O_2 content in dry flue gas	Volume fraction	0.084
Flue gas recirculation ratio		0.3
Fuel characteristics		
C	Mass fraction d.b.	0.483
H	Mass fraction d.b.	0.059
O	Mass fraction d.b.	0.43
N	Mass fraction d.b.	0.0034
Moisture content	Mass fraction w.b.	0.154
Ash	Mass fraction d.b.	0.022
NCV	$kJ\ kg^{-1}$ w.b.	14.86
GCV	$kJ\ kg^{-1}$ d.b.	19.31

Explanations: w.b.: wet basis; d.b.: dry basis; GCV: gross calorific value; NCV: net calorific value.

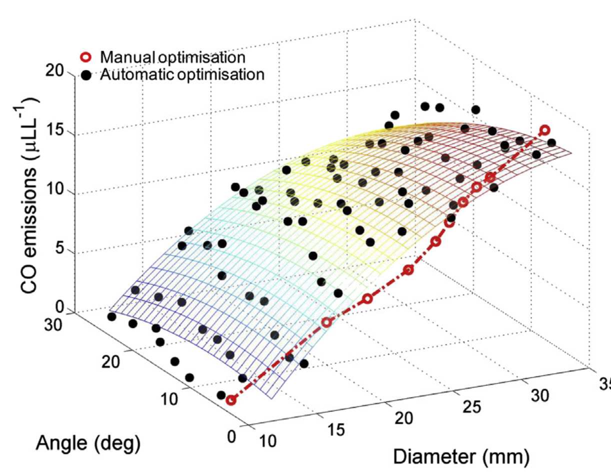

Fig. 2 – Response surface plot of CO emissions calculated with the automatic optimisation method.

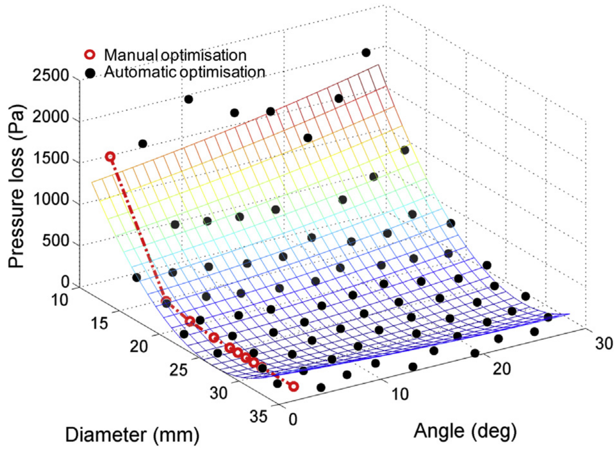

Fig. 3 – Response surface plot of pressure losses calculated with the automatic optimisation method.

difference between the minimum and the maximum of output variable divided by the average value of all the design points. They are obtained by varying one input parameter while holding the other input parameters constant. The larger the sensitivity of the output variables, the more significant the role of the input parameter is.

This analysis provides helpful information especially when there are more than two design parameters. Input design parameters with a low sensitivity can be skipped since they have no strong influence on the output variables. Therefore, within the automatic optimisation study the sensitivity analysis was performed to achieve a better understanding about the impact of the design parameters on the output variables.

Fig. 4 shows the local sensitivity of the pressure loss and CO emission regarding the change of the nozzles diameter and angle. The positive sign in the chart indicates that an increase of the design parameter increases the output variable as well, and vice versa.

It is shown from Fig. 4 that the diameter has a large (negative) impact on the pressure loss and a moderate positive impact on CO emission. This means that by increasing the diameter of the secondary air nozzles the pressure loss decreases while the CO emissions increase. The reduction of the diameter of the secondary air nozzles causes a higher gas velocity at nozzle exit. This results in a better mixing of secondary air with the flue gas due to a deeper penetration of the air jets into the flue gas which results in a higher net CO reaction rate. Furthermore, the pressure loss increases due to the higher kinetic energy loss with smaller nozzle diameters. Fig. 5 shows the dependency of CO emissions on the angle of the secondary air nozzles for different diameter ranges. The results show that the CO dependency on the angle is low for smaller diameters and increases for larger diameters. Furthermore, the sensitivity graph shows that the angle of secondary air nozzles has a moderately negative impact on CO emissions while it has a relatively high positive impact on the pressure loss. This implies that with an increasing angle the CO emissions slightly decrease and the pressure loss increases. Generally, the sensitivities of both output variables concerning the diameter and the angle variation have an opposite sign which indicates that theoretically the variation of the two input parameters could compensate the effect of each other when they are varied simultaneously and in the same direction. However, the sensitivities of the CO emissions and the pressure loss on the diameter are considerably larger than on the angle.

Fig. 6 shows the values of the weight function calculated according to equation (1) for different combinations of nozzle angles and diameters. By screening through the weight surface, many local minima can be detected. These local minima represent the smallest values in a certain investigated area, while the global minimum represents the smallest value within the total definition range of the variation parameters. The absolute minimum represents the optimum combination of nozzle diameter and nozzle angle (15 mm diameter and 5° nozzle angle in the present case). While in the automatic optimisation study the whole parameter range is investigated systematically, only a few simulations based on trial-and-error can be performed during a manual optimisation study. Therefore, the automatic optimisation provides considerably higher possibility to find the global optimum.

In Fig. 7 the CO emissions are plotted against the pressure loss for all design points. Here, the Pareto front represents the design points which have the lowest CO emission for a chosen pressure loss and the lowest pressure loss for a chosen CO emission, respectively. Hence, by the Pareto front not only the global optimum can be found but also the best possible design for a certain restriction e.g. concerning the pressure loss.

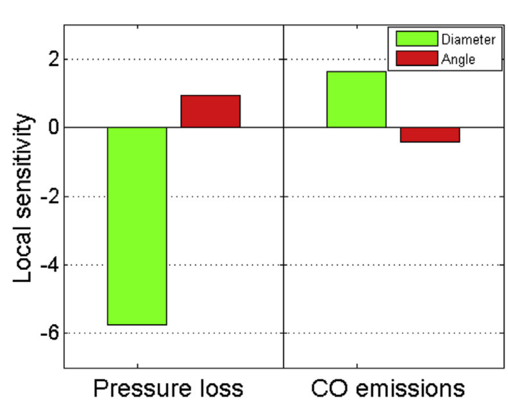

Fig. 4 – Sensitivity diagram of the impact of the design parameters on the output variables.

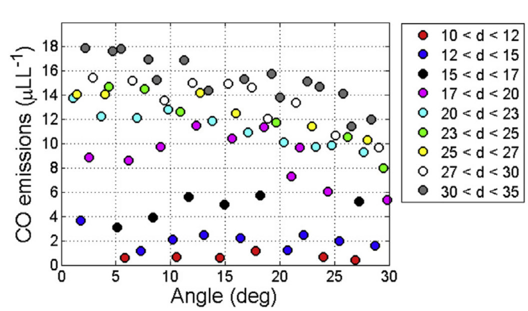

Fig. 5 – Dependence of CO emissions on the angle of secondary air nozzles for different diameter ranges.

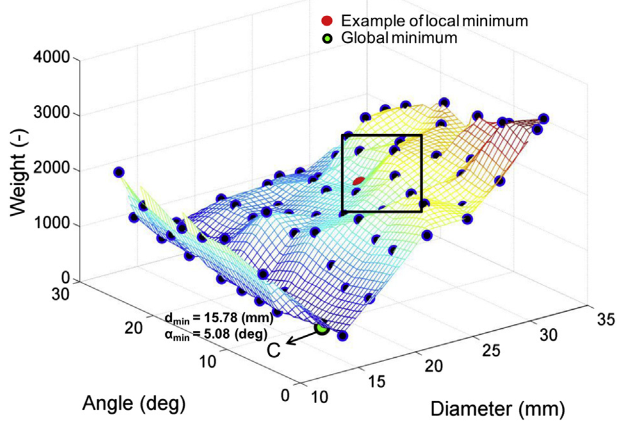

Fig. 6 – **Weight surface from automatic optimisation calculated based on 80 design points (tetrahedral mesh type with 1 million grid cells).**

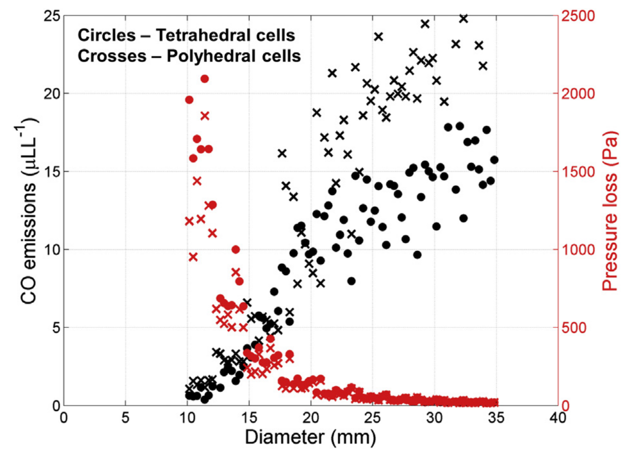

Fig. 8 – **Effect of mesh type on the calculated CO emissions and pressure losses for the pilot-scale grate furnace.**

Additionally, a further automatic parameter study has been carried out to investigate the influence of the grid type on computation time and accuracy. For this purpose, two sets of grid have been studied: a tetrahedral mesh and a polyhedral mesh. While the first grid type has been used as reference grid with 1 million cells (high resolution), the polyhedral type was generated by a conversion of the tetrahedral mesh type. This method reduces the number of mesh cells to approximately 250,000 cells.

The influence of the different grids on the results is shown in Fig. 8. The CO emission calculated with the polyhedral mesh shows deviations from results which have been achieved with the tetrahedral mesh for diameters larger than 20 mm, since the penetration of the secondary air is underestimated due to large cell sizes in the region of the nozzles. The calculated weight function for the different meshes is shown in Fig. 9. While for a diameter of approximately 15 mm the pressure drop is below 200 Pa, the CO concentration at the outlet of the secondary combustion chamber is still below 8 ($\mu L\,L^{-1}$) (see Fig. 8). Although the CO emissions calculated with the polyhedral mesh show deviations from the values calculated with the tetrahedral mesh, the optimum of the weight function (point H) is located approximately at the same position (point G) (see Fig. 9). The main reason for the difference between the obtained global minimum from the manual optimisation study (point K) in comparison to the automatic optimisation studies (points G and H) is due to the effect of angle variations which has not been considered in the manual study.

In case of the tetrahedral mesh type the overall optimisation time took one month under consideration of two optimisation parameters (diameter and angle for 80 design points). By using the polyhedral mesh, the optimum of the parameter study was found within 6 days. In contradiction, a manual design study would need approximately 8 months due to the comprehensive number of person-hours to create the numerical grid and to set-up the calculations for each design point.

Despite deviations in CO emission predictions from the reference grid, the polyhedral mesh shows a great potential to accelerate the optimisation cycle. A local mesh refinement in

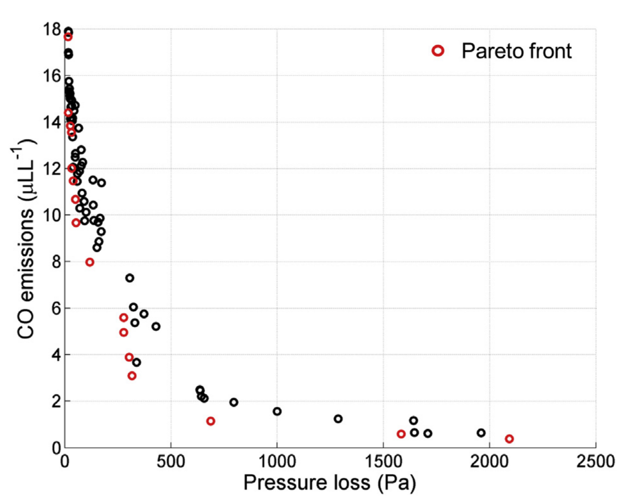

Fig. 7 – **Results for design points with Pareto front.**

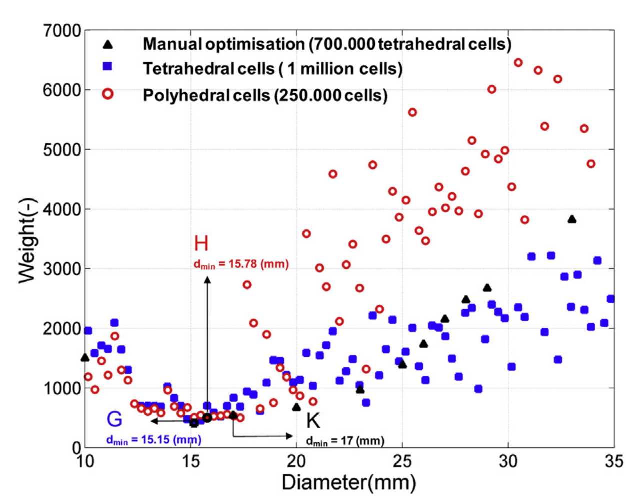

Fig. 9 – **Weight function for different mesh types.**

the region of secondary air jets is needed for an improved CO prediction and is expected to just slightly increase the mesh size and hence computation time.

4. Summary and conclusions

A new automatic optimisation routine was developed and tested for a biomass pilot-scale grate furnace concerning the minimisation of CO emissions and pressure loss. The sensitivity analysis performed underlines the high impact of the nozzle diameter on the pressure losses and CO emissions in comparison to the nozzle angle. The parameter variation performed automatically is by far more efficient than the manual case study due to the considerably lower simulation time and personnel demand. The overall simulation time for the calculation of 80 design points could be reduced by a factor of 8 in case of the tetrahedral mesh type and by a factor of 32 in case of the polyhedral mesh type. Although the CO emission trends were slightly differing for the two studied grid types, the global minima are located nearly at the same positions. However, the prediction accuracy of the coarser polyhedral mesh can be further improved at an acceptable increase of computational time by a further increased local mesh refinement near the secondary air nozzles. Concluding, the new CFD optimisation routine proofed to work efficiently in terms of nozzle design optimisation and time demand. In future it shall be further extended to geometry optimisation issues as well as the automatic simulation of different operating conditions for a defined geometry as a basis for an improved process control.

REFERENCES

[1] Safikhani H, Hajiloo A, Ranjbar M, Nariman-Zadeh N. Modeling and multi-objective optimisation of cyclone separator using CFD and genetic algorithms. Comput Chem Eng 2011;35(6):1064–71.

[2] Elsayed K, Lacor C. Modeling, analysis and optimisation of aircyclones using artificial neural network, response surface methodology and CFD simulation approaches. Powder Technol 2011;212(1):115–33.

[3] Safikhani H, Akhavan-Behabadi MA, Nariman-Zadeh N, Abadi MJM. Modeling and multi-objective optimisation of square cyclones using CFD and neural networks. Chem Eng Res Des 2011;89(3):301–9.

[4] Elsayed K, Lacor C. Optimisation of the cyclone separator geometry for minimum pressure drop using mathematical models and CFD simulations. Chem Eng Sci 2010;65(22): 6048–58.

[5] Sungwook P. Optimisation of combustion chamber geometry and engine operating conditions for compression ignition engines fueled with dimethyl ether. Fuel 2012;97:61–71.

[6] Sungwook P. Optimisation of combustion chamber geometry for stoichiometric diesel combustion using a micro genetic algorithm. Fuel Process Technol 2010;91(11):1742–52.

[7] Derakhshan S, Mohammadi B, Nourbakhsh A. Incomplete sensitivities for 3D radial turbo machinery blade optimisation. Comput Fluids 2008;37(10):1354–63.

[8] Derakhshan S, Mohammadi B, Nourbakhsh A. The comparison of incomplete sensitivities and genetic algorithms application in 3D radial turbo machinery blade optimisation. Comput Fluids 2010;39(10):2022–9.

[9] Kim K, Seo S. Application of numerical optimisation technique to design of forward curved blades centrifugal fan. JSME Int J Ser B 2006;49(1):152–8.

[10] Huai HL, Xu WL, Qu ZY, Li ZG, Zhang FP, Xiang GM, et al. Analysis and optimisation of municipal solid waste combustion in a reciprocating incinerator. Chem Eng Sci 2008;63:3100–13.

[11] Shah KV, Vuthaluru R, Vuthaluru HB. CFD based investigations into optimisation of coal pulveriser performance: effect of classifier vane setting. Fuel Process Technol 2009;90:1135–41.

[12] Scharler R, Benesch C, Schulze K, Obernberger I. CFD simulations as efficient tool for the development and optimisation of small-scale biomass furnace and stoves. In: Faulstich M, editor. 19th European biomass conference & exhibition; June 2011; Berlin; Germany. Florence; Italy: ETA-Renewable Energies; 2011. p. 4–12.

[13] Scharler R. Entwicklung und Optimierung von Biomasse-Rostfeuernungen durch CFD-Analyse. PhD Thesis. Graz University of Technology; 2001.

[14] Widmann E. Modellbildung zum Abbrandverhalten von Biomasse unter besonderer Berücksichtigung der N-Freisetzung am Beispiel einer Rostfeuerung. MSc Thesis. Graz University of Technology; 2002.

[15] Scharler R, Widmann E, Obernberger I. CFD modeling of NO_x formation in biomass grate furnaces with detailed chemistry. In: Bridgwater AV, Boocock DGB, editors. Science in thermal and chemical biomass conversion; Sept 2004. Victoria; Canada. UK: CPL Press; 2006. p. 284–300.

[16] Scharler R, Benesch C, Neudeck A, Obernberger I. CFD based design and optimisation of wood log fired stoves. In: De Santi GF, editor. 17th European biomass conference & exhibition; June 2009; Hamburg; Germany. Florence; Italy: ETA-Renewable Energies; 2009. p. 1361–7.

[17] Scharler R, Fleckl T, Obernberger I. Modification of a Magnussen constant of Eddy dissipation model for biomass grate furnaces by means of hot gas in-situ FT-IR absorption spectroscopy. Prog Comput Fluid Dyn Int J 2003;3:102–11.

[18] Scharler R, Forstner M, Braun M, Brunner T, Obernberger I. Advanced CFD analysis of large fixed bed biomass boilers with special focus on the convective section. In: van Swaaij WPM, editor. 2nd World conference and exhibition on biomass for energy, industry and climate protection; May 2004; Rome; Italy. Florence; Italy: ETA-Renewable Energies; 2004. p. 1357–60.

[19] Scharler R, Obernberger I. CFD analysis of air staging and flue gas recirculation in biomass grate furnaces. In: Kyritsis S, editor. 1st World conference on biomass for energy and industry; June 2000; Sevilla; Spain. London, UK: James&James (Science Publishers) Ltd.; 2001. p. 1935–9.

[20] Magnussen BF, Hjertager BH. On mathematical modeling of turbulent combustion with special emphasis on soot formation and combustion. In: 16th Symp (Int) combust; August 1976; Massachusetts Institute of Technology; Cambridge; Massachusetts; USA. Pittsburgh; PA; USA: The Combustion Institute; 1977. p. 719–29.

[21] Brink A. Eddy Break-Up based models for industrial diffusion flames with complex gas phase chemistry. PhD Thesis. Abo Akademi University; 1998.

[22] ANSYS®. Academic research, release 14.0, help system, design exploration user guide. ANSYS, Inc.